

Chapter IV
ELECTRICAL CONDUCTIVITY

CHAPTER - IV

ELECTRICAL CONDUCTIVITY

I INTRODUCTION :

A semiconductor is often defined as an electrical conductivity intermediate between that of an insulator and a metal. The properties of semiconductors which are generally termed as their electrical properties include (1) Electrical conductivity, (2) The Hall coefficient which determines the carrier density and type (3) Hall mobility of the charge carriers under the influence of transverse electric field and magnetic field (4) Many semiconductors change their resistance when subjected to magnetic field, the effect being known as magneto-resistivity. In this case, usually the fractional change of the resistivity $\Delta \rho / \rho_0$ in the magnetic field with respect to zero field value is obtained, (5) The thermoelectric power of a semiconductors is often useful. When a temperature difference is maintained between the ends of the specimen, there arises an EMF across the two ends and it is measured in mV/°C. Among these, the electrical conductivity is the most commonly measured property. The electrical conductivity of the vacuum deposited and heat treated thin films can give important information regarding the defect structure and density of defects present in the as-grown thin films and can throw light

on the changes that take place during annealing process in the film. It is also possible to study the influence of deposition parameters on the defect density and structure of thin films by the conductivity measurements.

In the present study, the resistivity of the bulk was measured by Valde's technique⁽¹⁾ of four point-contact array and for thin films, the usual four probe method described by Goswami⁽²⁾ has been used.

The effect of the various growth conditions and heat treatments on the electrical conductivity of the bulk and thin films has been studied. The Hall measurements have also been carried out.

Bhatt et al⁽³⁾ have measured the electrical properties of the crystals grown by Bridgman Stockbarger technique. The conductivities of crystals of SnSe and SnSe₂ have been reported to be about $15(\text{ohm-cm})^{-1}$ and $2.05(\text{ohm-cm})^{-1}$, respectively. Yu et al⁽⁴⁾ have measured electrical properties of vapour transport grown SnSe single crystals. They found that these crystals have an average hole concentration of about 10^{18} cm^{-3} and mobility about $154\text{ cm}^2/\text{Vs}$ at room temperature. Domingo et al⁽⁵⁾ measured electrical properties of vapour grown SnSe₂ crystals and found the electrical conductivity to be $3.6(\text{ohm-cm})^{-1}$, the electron concentration 10^{18} cm^{-3} and mobility $27\text{ cm}^2/\text{Vs}$. W. Albers⁽⁶⁾ measured the Hall mobility and carrier

concentration of SnSe crystals to be about $3 \times 10^{18} \text{ cm}^{-3}$ and $100 \text{ cm}^2/\text{Vs}$, respectively, and for SnSe_2 , $2 \times 10^{18} \text{ cm}^{-3}$ and $10 \text{ cm}^2/\text{Vs}$ respectively. Dang Tran Quan ⁽⁷⁾ measured the resistivity and Hall coefficient of directly evaporated thin films from the SnSe compound. He found that the resistivity decreases with the increasing temperature, whereas the Hall mobility and carrier concentration increase with increasing temperature. Further, an exponential $1/T$ law was observed for each of these variations. The results have been explained in terms of grain boundary potential barrier mechanism. Dang Tran Quan ⁽⁸⁾ has also reported studies on the solid state reacted SnSe films. The resistivity, Hall mobility and the carrier concentration are reported to be about 8 ohm-cm , $59 \text{ cm}^2/\text{Vs}$ and $9.5 \times 10^{16} \text{ cm}^{-3}$, respectively.

II GENERAL DISCUSSION :

Several theories have been developed connecting electrical conductivity changes due to annealing, defects and grain boundaries. For example, Valde's ⁽¹⁾ theory has been extensively used for the analysis of electrical conductivity data of annealed films to study the defect structure of vacuum deposited thin films. According to quantum theory, electrical conduction in metals is due to electrons, while electrical resistivity results from the scattering of these electrons by the lattice. Because of their wave nature, electrons can pass through a perfect lattice without any attenuation. Actually no

lattice is perfect. Electrons always undergo some scattering as they move through a solid, the average distance that they travel between successive collisions being called the mean free path (mfp)⁽⁹⁾. Bloch showed that the mfp of an electron travelling through a perfect rigid lattice is infinite. In other words the electron can move without resistance in a perfect lattice. But lattice imperfections present in real samples give rise to electrical resistivity. Impurity atoms, vacancies, dislocations, grain boundaries and stacking faults are static defects while the dynamic imperfections are due to thermal motion of the atoms in the lattice. The vibrational modes of atoms are quantized and are called phonons. The number of phonons in a given lattice increases with temperature causing increasing electron-phonon collisions with increasing temperature and hence the resistivity increases according to the relation

$$\rho_0 = \rho_{ph}(T) + \rho_i \quad \dots 1$$

where ρ_0 = total resistivity, ρ_{ph} = temperature dependent resistivity due to phonons and ρ_i = resistivity due to impurities.

Normally the dimensions of bulk conductors are of several orders of magnitude larger than the mfp of conduction electrons. Hence the number of surface collisions are very

small compared to the total number of collisions taking place in the bulk. However, the surface collisions cannot be neglected if one or more dimensions of the conductor approaches to or are less than the mfp, as in the case of thin films. Polycrystalline films are made up of small single crystals in contact with one another. Except for the size, the crystallites in polycrystalline films should be similar to larger single crystals. However, the additional scattering due to grain boundaries will reduce the effective carrier mobility compared to the bulk value and hence the measurements of electronic properties of films should yield results which represent the average of contributions of the crystallites and the grain boundaries as well as the average of anisotropies of the randomly oriented grains. As the size of the grains becomes smaller, the role of the grain boundaries becomes more important and the material begins to resemble an amorphous solid. Thus, an estimate of the maximum possible contribution to the resistivity from the grain boundaries may be arrived at by considering the resistivities of liquid metals. In the case of films, electrical resistivity depends on the growth stages and the film may be granular or island-like porous (network) or continuous. Each stage has its characteristic electrical properties.

Electrical conductivity of a granular film is of many orders of magnitude smaller than that of the bulk material and

is generally characterized by a negative temperature coefficient of resistivity. The conductivity is found to vary exponentially with the inverse of temperature. As the thickness of film becomes comparable in magnitude with the mfp of the carriers, the film boundaries impose a limitation on the movement of the carriers, and thus the effective value of mfp. Physical effects arising because of this geometrical limitation on the mfp are termed as "mean free path" or "size" effects. Size effects in a film can also be studied by varying the mfp instead of the film thickness. This is achieved by a study of the temperature dependence of the film resistivity. At low temperatures, $T < \Theta_D$, where Θ_D is the Debye temperature, the mfp of the electrons in thin films may not be the same as that in the bulk. Further, because of the longer free path available at low temperatures, small angle electron phonon scattering is very effective. (10)

In the case of semiconductors, for a particular range of temperature, the density of conduction electrons increases with temperature. This is because of the thermally activated transition of more and more electrons from donor levels to the conduction band or holes from the acceptor levels to the valence band. The energy required for this process is known as the resistivity activation energy. The conductivity is found to vary exponentially with the inverse of temperature. The smaller the size of the particles (grains), the greater is the

activation energy. The larger the distance between the particles, the lower is the tunneling probability. In both the cases, the conductivity is lowered. The size of the particles and inter-particle separation are generally relatively greater for a lower melting point of the deposit material, a higher substrate temperature and a smoother substrate. Thus, given the deposition conditions, one can predict the conduction behaviour of granular films.

Many conventional methods for measuring resistivity are unsatisfactory for semiconductors because metal-semiconductor contacts are usually rectifying in nature. Also there is generally minority carrier injection by one of the current carrying contacts. An excess concentration of minority carriers will affect the potential of the other contacts and modulate the resistance of the material.

The four probe methods have overcome these difficulties and also offer several other advantages. They permit measurements of resistivity in samples having a wide variety of shapes, including the resistivity of small volumes within bigger pieces of the semiconductor. In a single crystal material, the resistivity may vary smoothly from point to point. Often, however, it is conventionally stated that it is constant within small percentage and when the variation does in fact fall within this tolerance, it is ignored. Soldered probe contacts may disturb the current flowing in the sample, shorting out part of

the sample and add to the ambiguity in the measurement of the probe spacing. Soldering directly to the body of the sample can affect the sample properties by heating and by contamination.

For determining the carrier concentration normally the Hall effect is used. When a conductor is placed in a magnetic field perpendicular to the direction of current flow, a field E_y is developed across the specimen in the direction perpendicular to both the current, J_x , and the magnetic field, H_z . The field, called the "Hall field", is given by

$$E_y = \frac{J_x H_z}{ne} \quad \dots 2$$

where J_x is the current density and n is the number of carriers per unit volume. Thus the Hall field is proportional to the product of the current density and the magnetic flux density. The proportionality constant, R_H , known as the Hall coefficient is given by

$$R_H = \frac{E_y}{J_x H_z} = \frac{1}{ne} \quad \dots 3$$

The product of Hall field and width of the film (i.e. dimension parallel to the field) is known as the Hall voltage. A

measurement of the Hall voltage for a known current and magnetic field yields a value of carrier concentration. The measurement of the sign of the Hall voltage is a common technique for determining if the sample is p-type or n-type.

III EXPERIMENTAL RESULTS :

Resistivity of the crystal and thin films :

Valde's four probe method has been used for the measurement of electrical conductivity of the crystals. The advantage of this technique is that one can use samples of any arbitrary shape. The problems of contact resistance and heating effect and contamination are avoided by using pressure contacts. A schematic of the contact array is shown in the Figure - 1.

A freshly cleaved sample with thickness approximately 0.5 mm was kept on the base plate of the sample holder. The four probes were allowed to rest under spring pressure on the middle of the sample. The current was adjusted to a desired constant value, I , through the two outer probes and the corresponding voltage, V , across the inner pair was measured. The whole set up was kept in an oven. The rate of heating was kept at about $5^{\circ}\text{C}/\text{min}$. The temperature was sensed by a thermometer of least count 1°C . The average distance between the successive probes was 2 mm. The resistivity is then calculated as :

$$\rho_0 = \frac{V}{I} \times 2 \pi S \quad \dots 4$$

where S = mean probe separation, ρ_0 = resistivity. Since the sample thickness was not too larger than the probe separation, a correction factor has to be applied giving resistivity to be

$$\rho = \frac{\rho_0}{G_7(w/s)} \quad \dots 5$$

where w = thickness of the sample and the correction factor $G_7(w/s)$ was obtained from the table for the appropriate value of $(w/s)^{(1)}$.

In the case of the thin film, since the resistance is usually high, Van der Pauw⁽¹¹⁾ method is not practical due to small value of voltage which cannot be measured accurately using a microvoltmeter. So the linear four probe method described by Goswami⁽²⁾ (Figure - 2) was used. The samples were prepared with rectangular geometry with a pre-evaporated aluminium film as the ohmic electrode. The length and breadth ratio of the film was kept more than 4 so as to avoid geometrical influence on the electrical characteristics. The resistivity was calculated using the formula.

$$\rho = \frac{Rwa}{l} \quad \dots 6$$

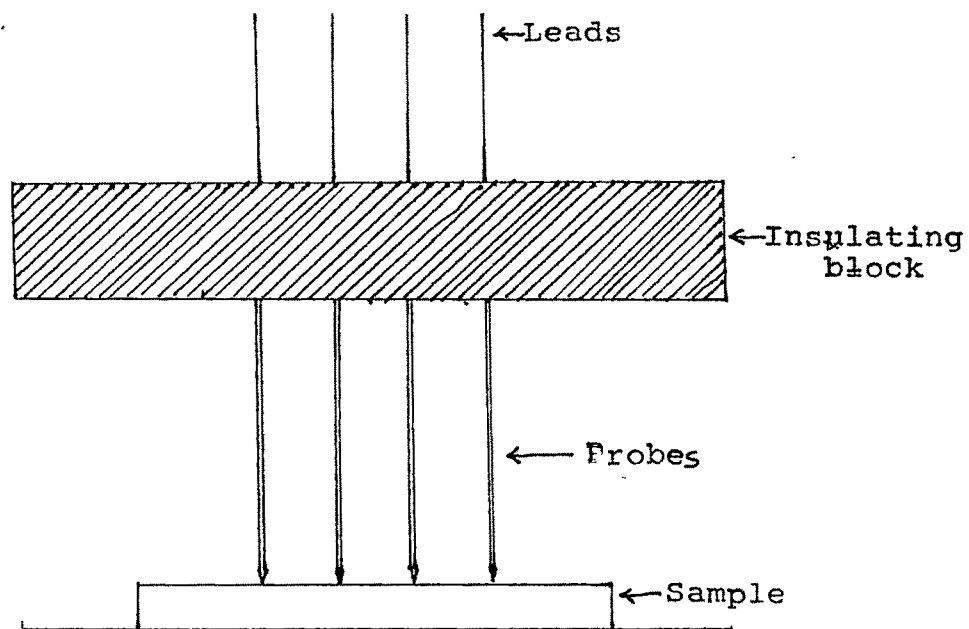


Figure - 1 : A schematic of the contact-array in Valde's set up.

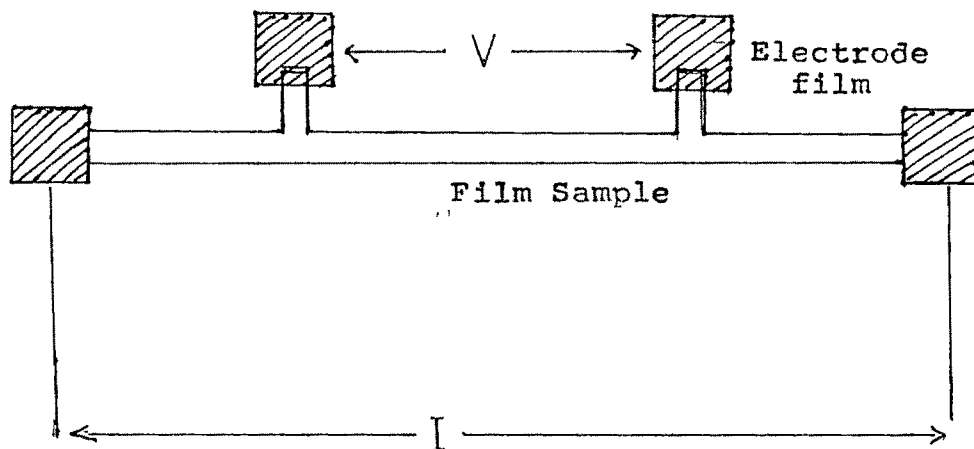


Figure - 2 : Linear four probe geometry.

where l is the length of the film, w is the width and a is the thickness of the film.

3.1 Resistivity of single crystals :

3.1.1 SnSe Crystal :

The room temperature resistivity of the SnSe single crystal was measured to be 0.210 ohm-cm. The observed temperature dependence is shown as a plot of $\ln \rho$ vs $1/T$ in Figure - 3. It is seen that the plot obeys the equation

$$\rho = \rho_0 \exp [-E_g/KT] \quad \dots 7$$

where E_g is the resistivity activation energy. The graph shows two linear regions, one from room temperature to 95°C and the other beyond 95°C. The activation energy values calculated from the corresponding slopes are found to be 0.036 eV and 0.11 eV, respectively. It is seen that with the increase in temperature, the resistivity increases upto a temperature of about 95°C. As the temperature increases beyond 95°C, the resistivity decreases. The resistivity shows exponential dependence on inverse of temperature. Thus the crystal displays intrinsic characteristic only above 95°C. Such a resistivity variation with temperature is explained by the presence of traps for electrons in the forbidden gap or by the formation of additional acceptors at high temperature (12,13,14).

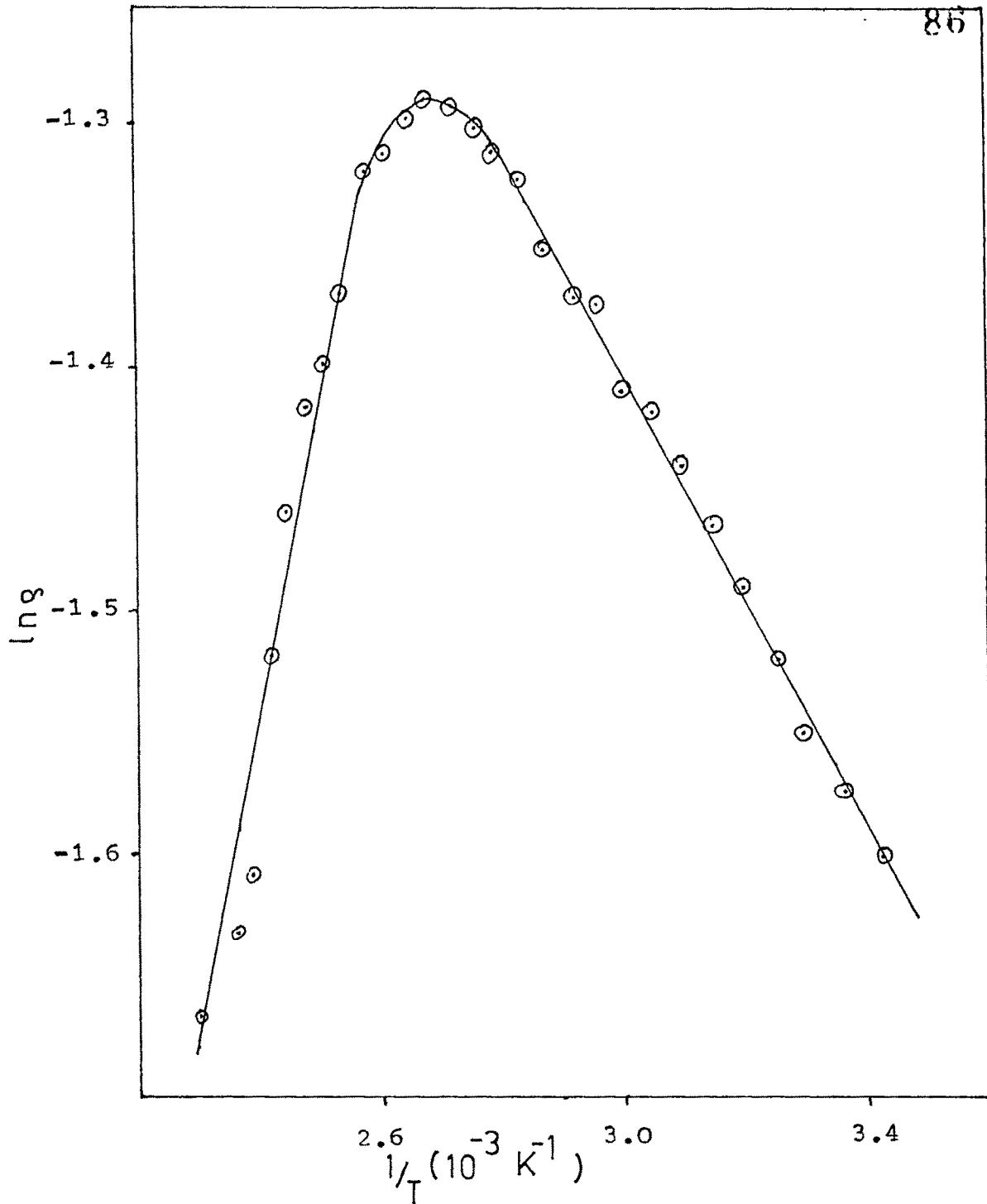


Figure - 3 : Plot of $\ln g$ vs $1/T$; SnSe Crystal.

3.1.2 SnSe₂ and SnSe-SnSe₂ eutectic crystals :

The resistivity of these crystals was measured at different temperatures. The $\ln \rho$ vs $1/T$ plots are shown in Figures - 4 and 5 for SnSe₂ and SnSe-SnSe₂ eutectic, respectively. A straight line is observed in both the cases implying the exponential dependence of resistivity on inverse temperature. The room temperature resistivity and activation energy for SnSe₂ crystals are found to be 0.41 ohm-cm and 5.18×10^{-3} eV respectively and for SnSe-SnSe₂ eutectic, they are found to be 9.03 ohm-cm and 0.072 eV, respectively.

The room temperature resistivity and activation energy measured for SnSe, SnSe₂ and SnSe-SnSe₂ eutectic crystals are given in Table - 1.

3.2 Electrical resistivity of thin films :

Resistivity of the thin films were studied by varying different parameters, namely, thickness, substrate temperature, nature of substrate, thermal cycling and heat treatment.

3.2.1 SnSe and SnSe₂ films directly evaporated from the compounds :

There has been a good amount of work on the electrical resistivity of these films reported in the literature^(15,16).

Handwritten notes and signatures at the bottom of the page, including the name "Chand" and other illegible markings.

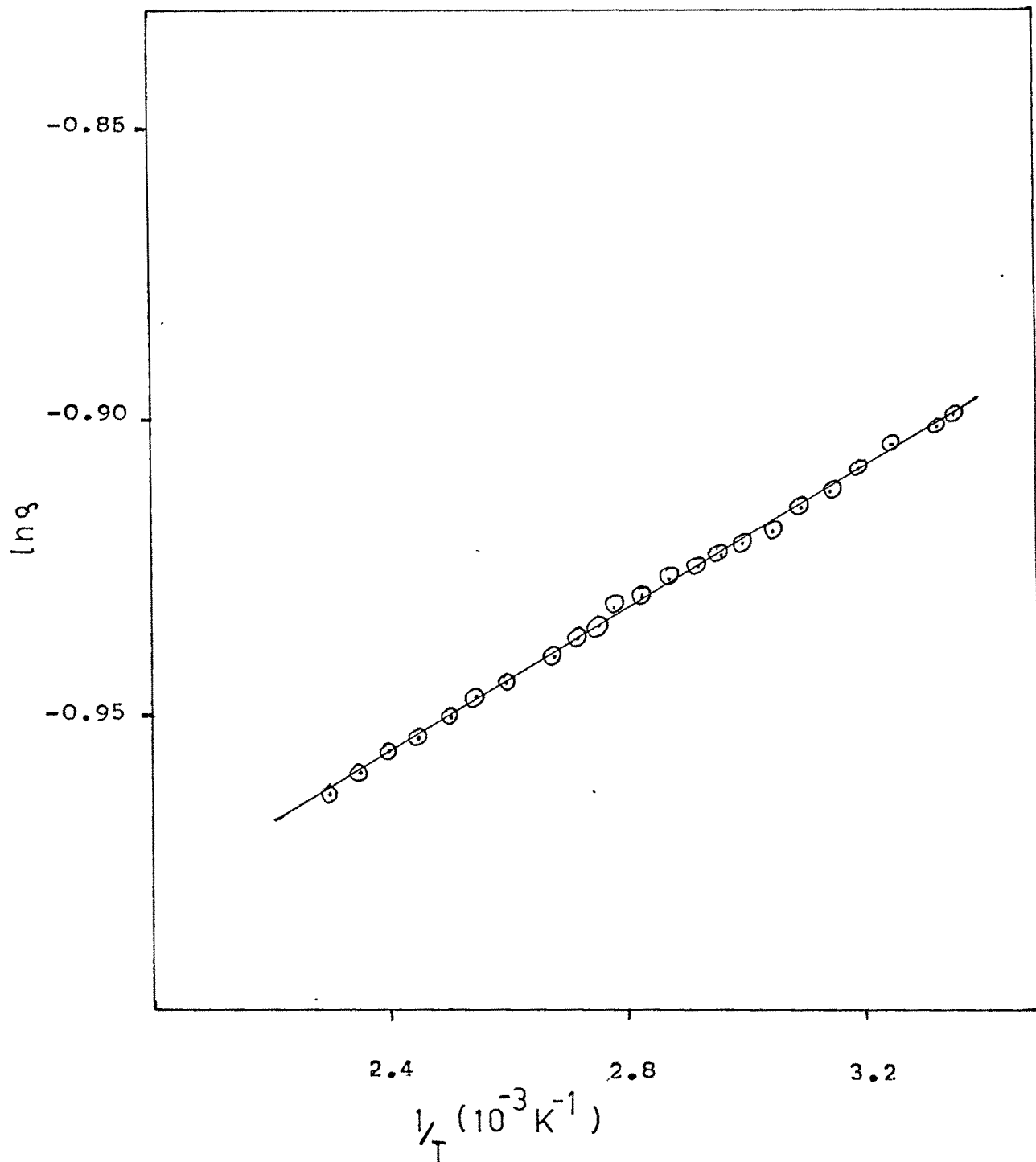


Figure - 4 : Plot of $\ln g$ vs $1/T$; SnSe_2 Crystal.

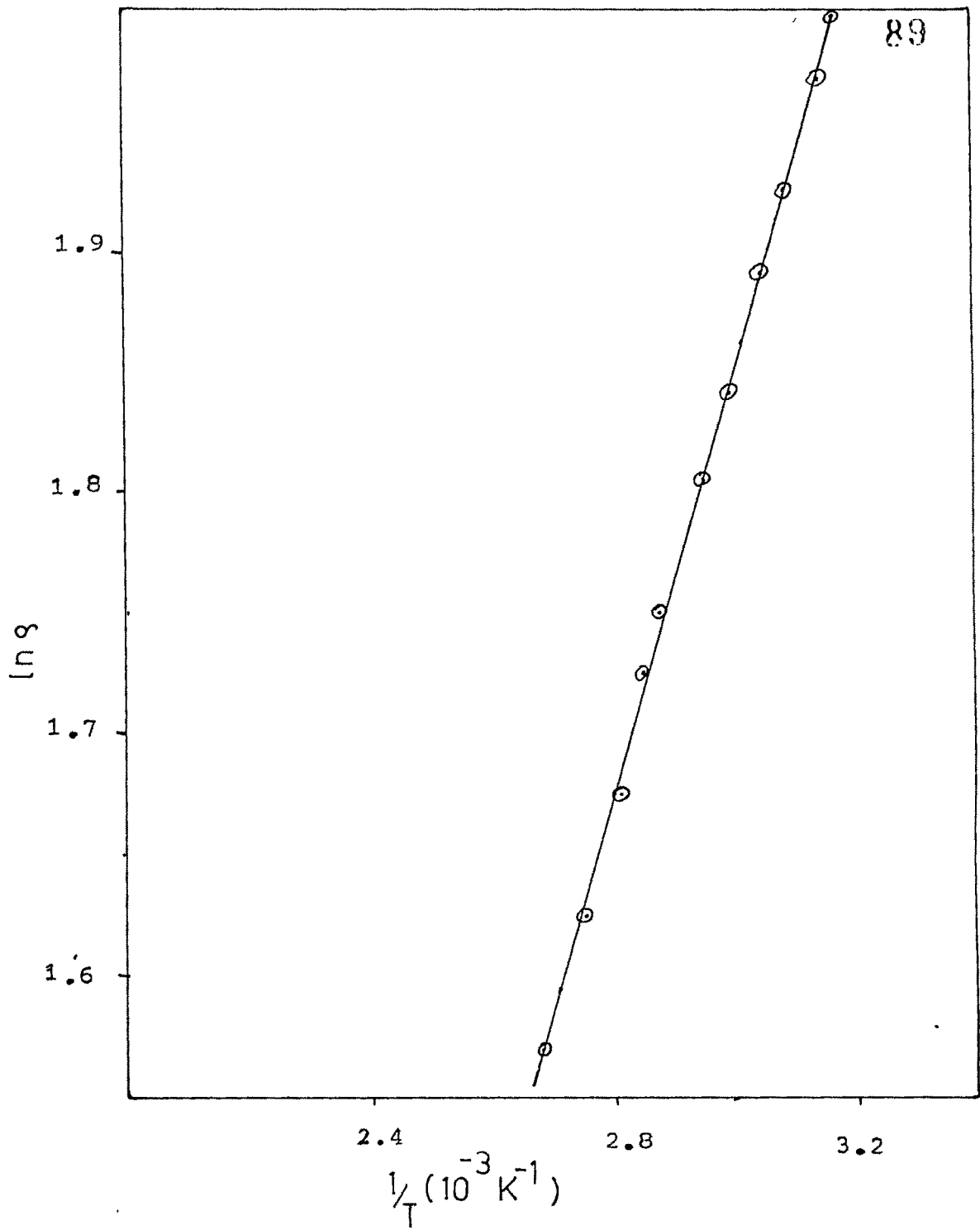


Figure - 5 : Plot of $\ln g$ vs $1/T$; SnSe-SnSe₂ eutectic crystal.

Films of SnSe of various thicknesses were deposited at 200°C substrate temperature following an earlier report that 200°C is the optimum temperature of deposition of SnSe so as to yield films of maximum crystallinity⁽¹⁷⁾. Therefore the SnSe films of different thicknesses were all obtained at the substrate temperature of 200°C. Their resistivities were measured at different temperatures. The plots of $\ln \rho$ vs $1/T$ of the films of different thicknesses are shown in Figure - 6. It is seen that the resistivity decreases with the increase in thickness. The room temperature resistivity and activation energy for different thicknesses are shown in Figures - 7 and 8 respectively.

In the case of SnSe₂, similar nature of resistivity variation with temperature was observed as shown in Figure - 9. It is a well known fact that the resistivity will respond to the change in mfp of the conduction electrons. Electrons will suffer a reflection at the surface when they happen to reach it. So the resistivity increases whenever the specimen is thin enough to favour the collision with the surface or in other words, upto particular thickness, the resistivity decreases with increasing thickness⁽¹⁸⁾. Moreover there will be an increase in grain size with increase in thickness.

SnSe₂ films were also deposited on different substrates, viz., (001) cleavage face of NaCl crystal, mica and glass. The plots of $\ln \rho$ vs $1/T$ for different substrates are of

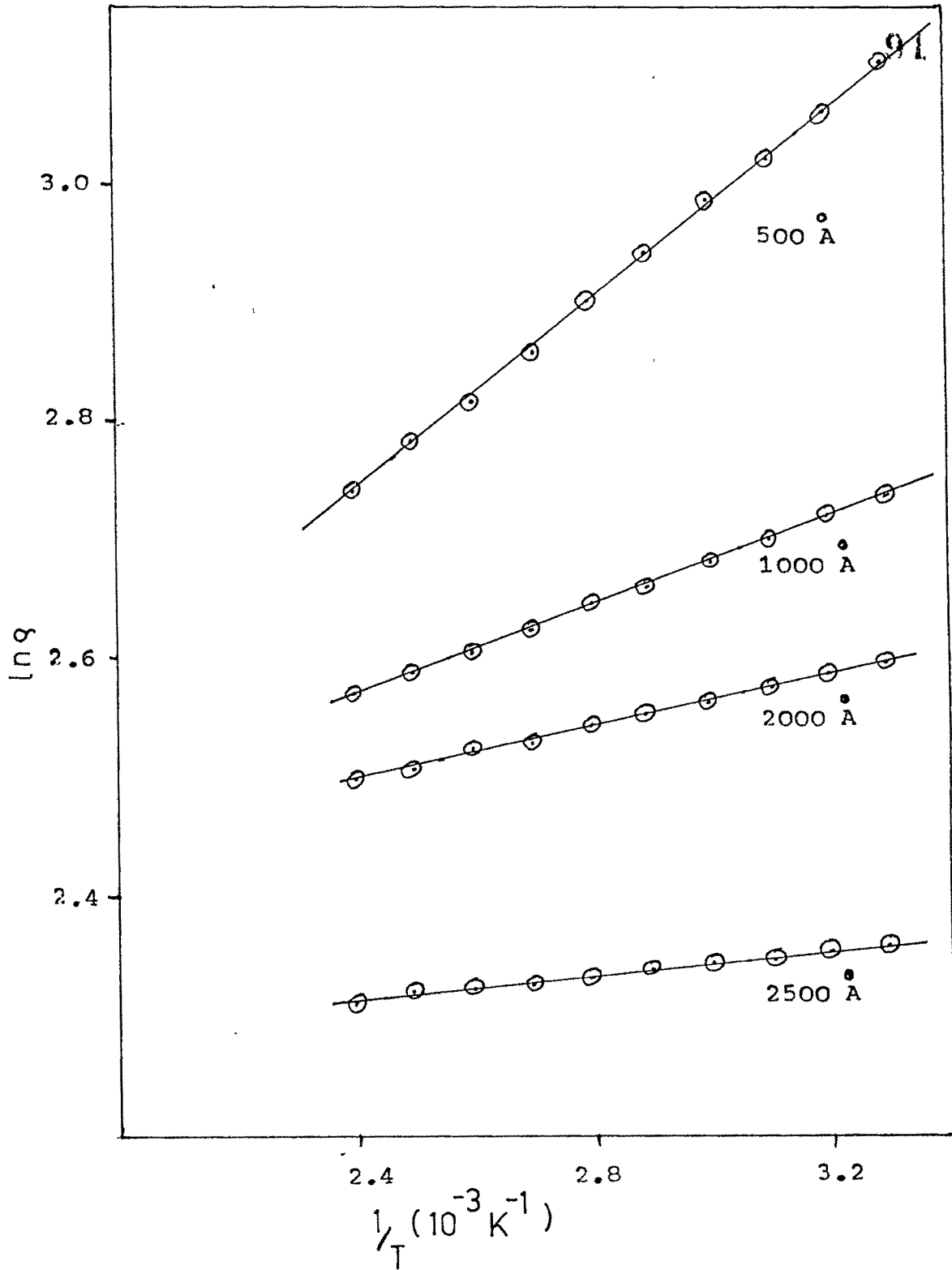


Figure - 6 : Plot of $\ln \eta$ vs $1/T$; SnSe films, of thicknesses indicated, deposited from the compound.
 (substrate temperature $\sim 200^\circ\text{C}$)

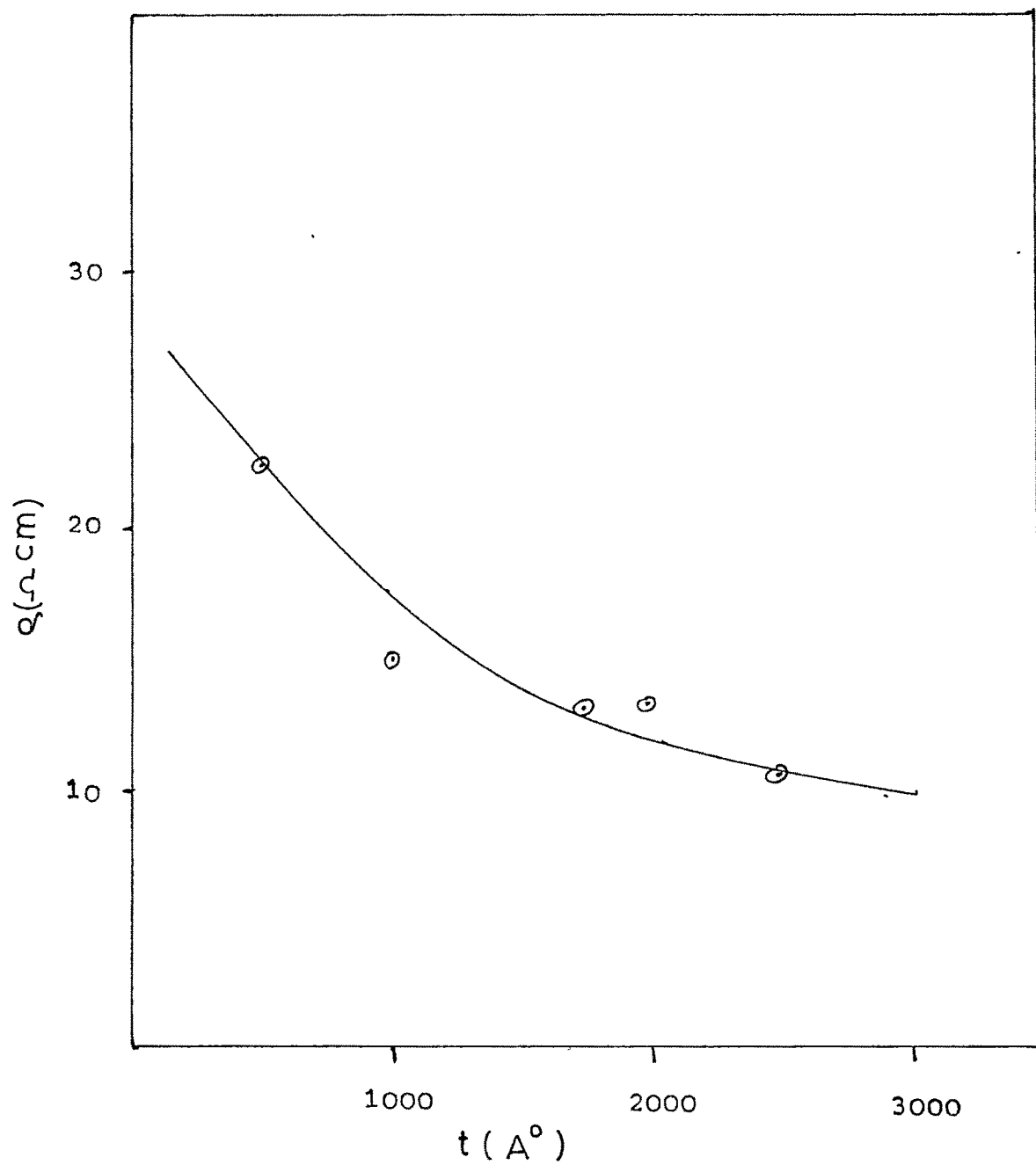


Figure - 7 : Plot of ρ vs t ; SnSe films directly evaporated from the compound.
(Substrate temperature 200°C)

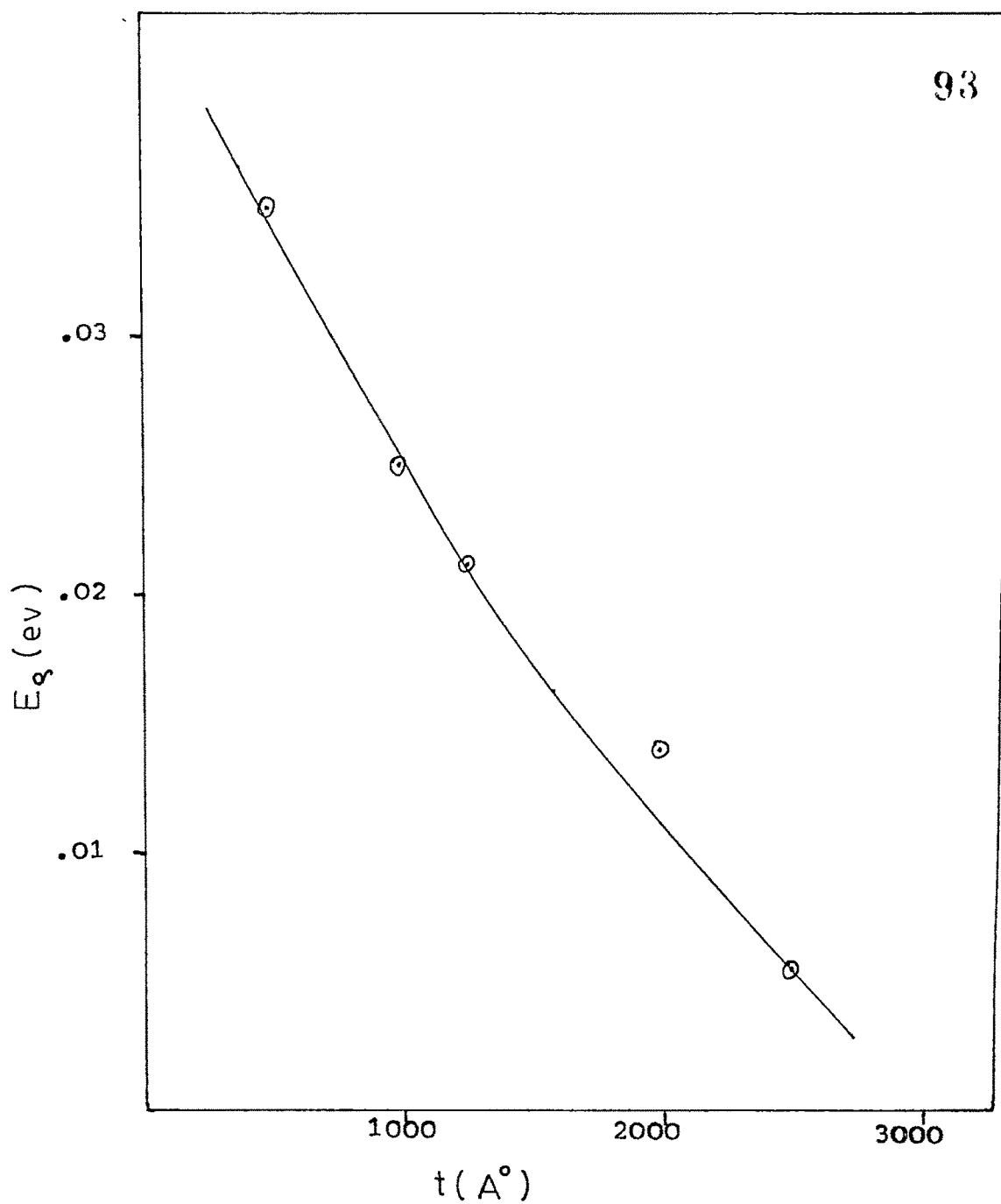


Figure - 8 : Plot of E_g vs t ; SnSe films directly evaporated film from the compound.

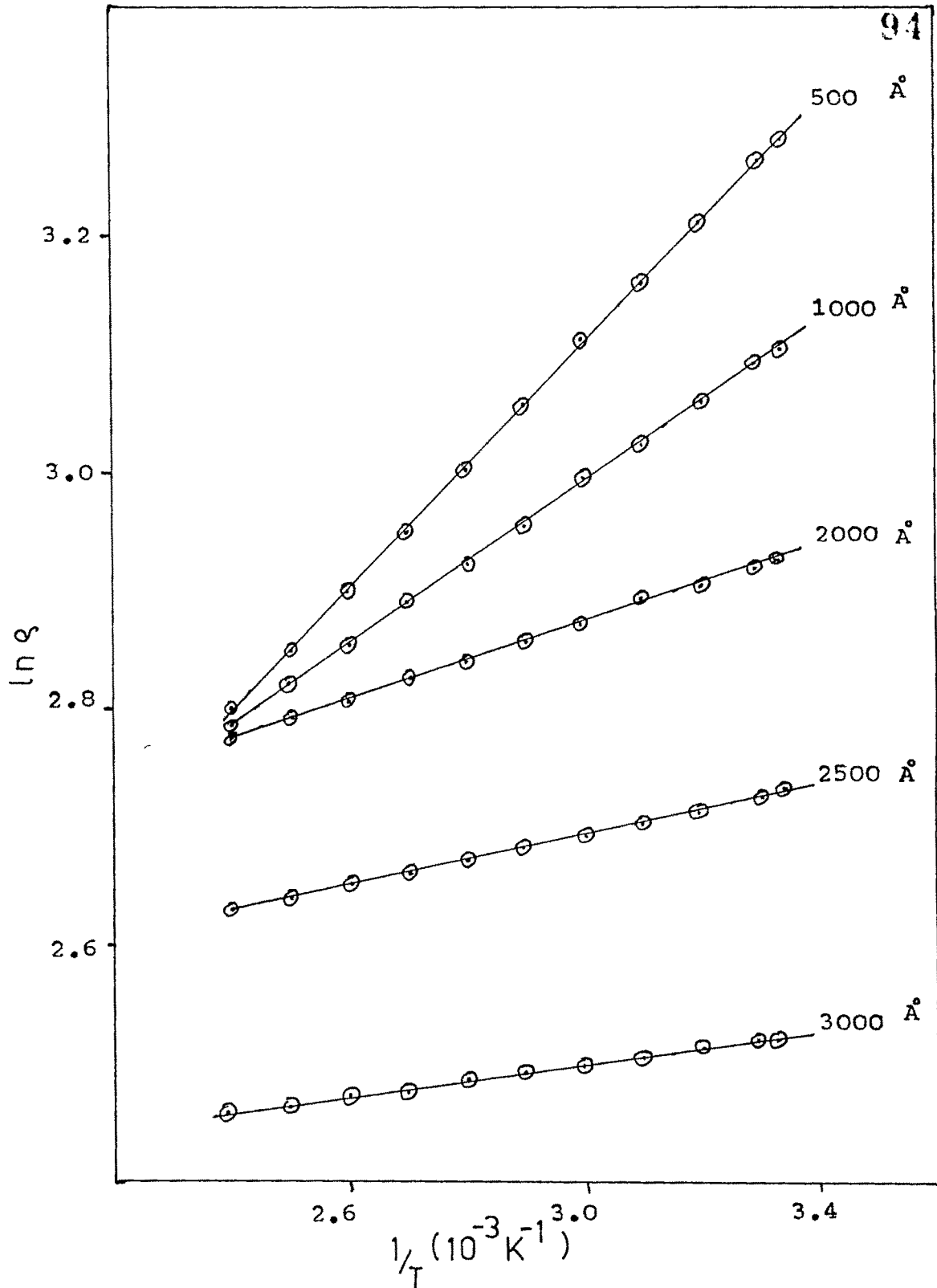


Figure - 9 : Plot of $\ln Q$ vs $1/T$; SnSe_2 films
of thicknesses indicated.
(Substrate temperature 200°C)

straight line nature, with negative slope, indicating the exponential dependence of resistivity on inverse temperature as expected. (Figure - 10). However, it is further seen that the films deposited on NaCl crystals have resistivity much lower than that of the films deposited on mica and glass substrate. Mica and NaCl are crystalline substrates while glass is amorphous. The crystallite size in the films also depends on the nature of the substrate. Some symmetry exists between the contacting planes of the two materials. The lattice parameters of SnSe₂ (hexagonal) are $a = 3.81 \text{ \AA}$ and $c = 6.14 \text{ \AA}$, those of NaCl (cubic) are $a = 5.63 \text{ \AA}$ and those of mica (monoclinic) are $a = 5.2 \text{ \AA}$ and $c = 10.3 \text{ \AA}$. Thus the parameters of SnSe₂ are in a closer matching with those of NaCl than with those of mica. Therefore epitaxy of SnSe₂ is better on the NaCl crystal than on mica. As a result, the SnSe₂ films on NaCl ought to have better crystallinity than the films on mica. This explains the lower resistivity of the films on NaCl substrates.

The values of room temperature electrical resistivity and activation energy obtained from $\ln \rho$ vs $1/T$ plots of SnSe₂ films are shown plotted against the film thickness in Figure - 11 and 12, respectively.

3.2.2 SnSe Solid State reacted films :

There has not been any work reported on this type of SnSe films except one report by Dang Tran Quan (1987)⁽⁸⁾.

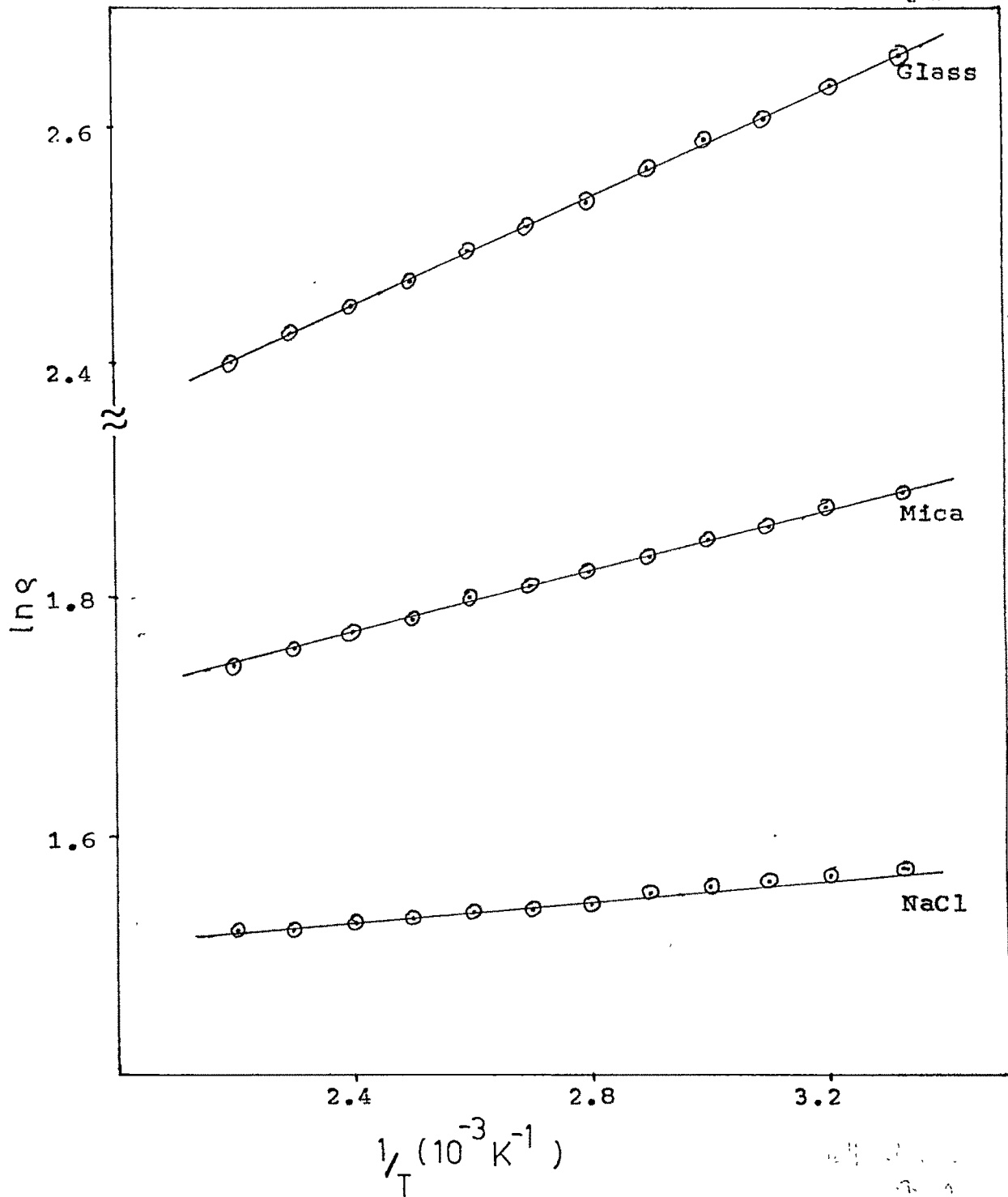


Figure - 10 : Plot of $\ln Q$ vs $1/T$ for the SnSe_2 films deposited on different substrates indicated

($t \sim 2000 \text{ \AA}$)

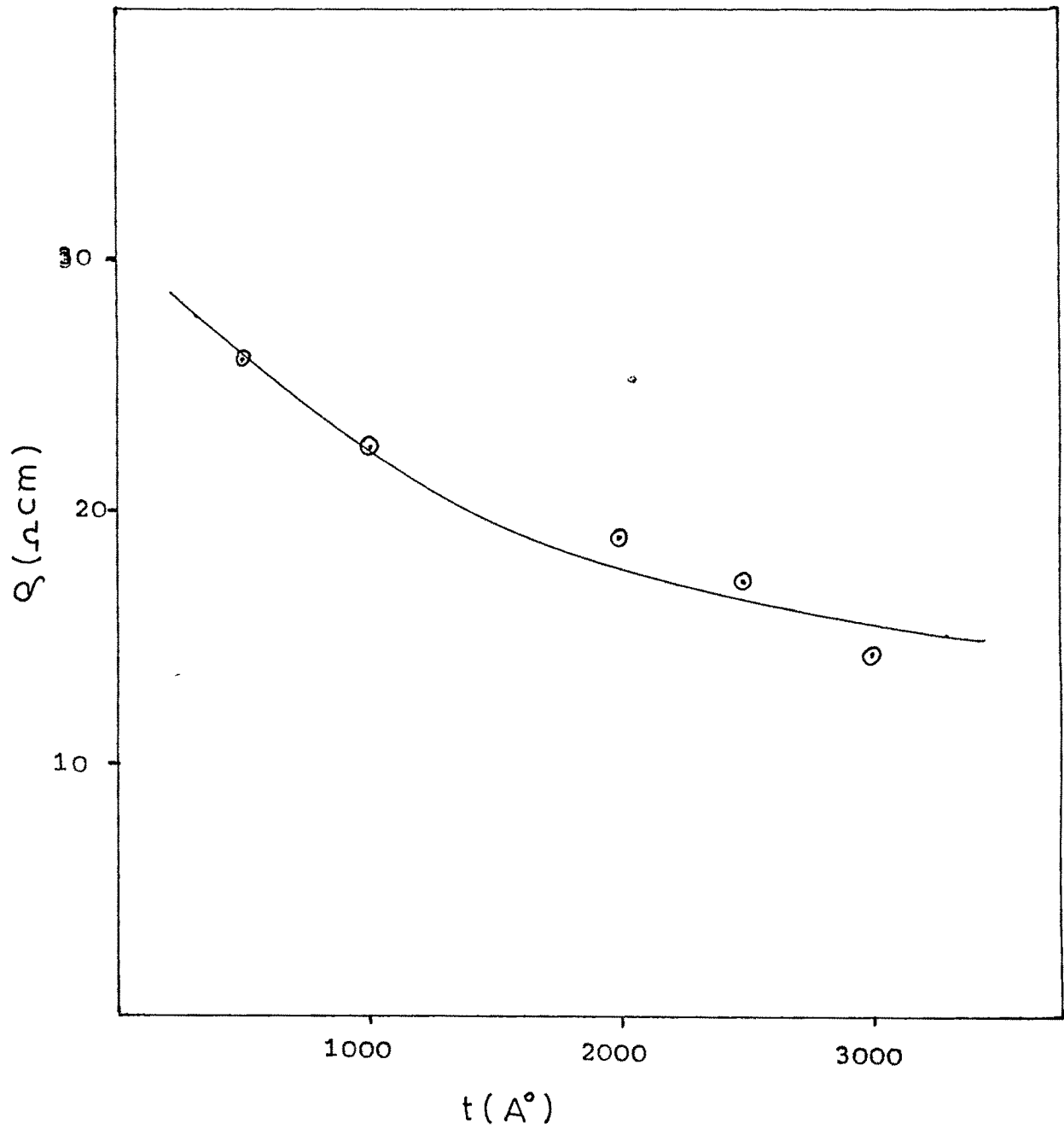


Figure - 11 : Plot of ρ vs t ; SnSe_2 films.
(substrate temperature 200°C)

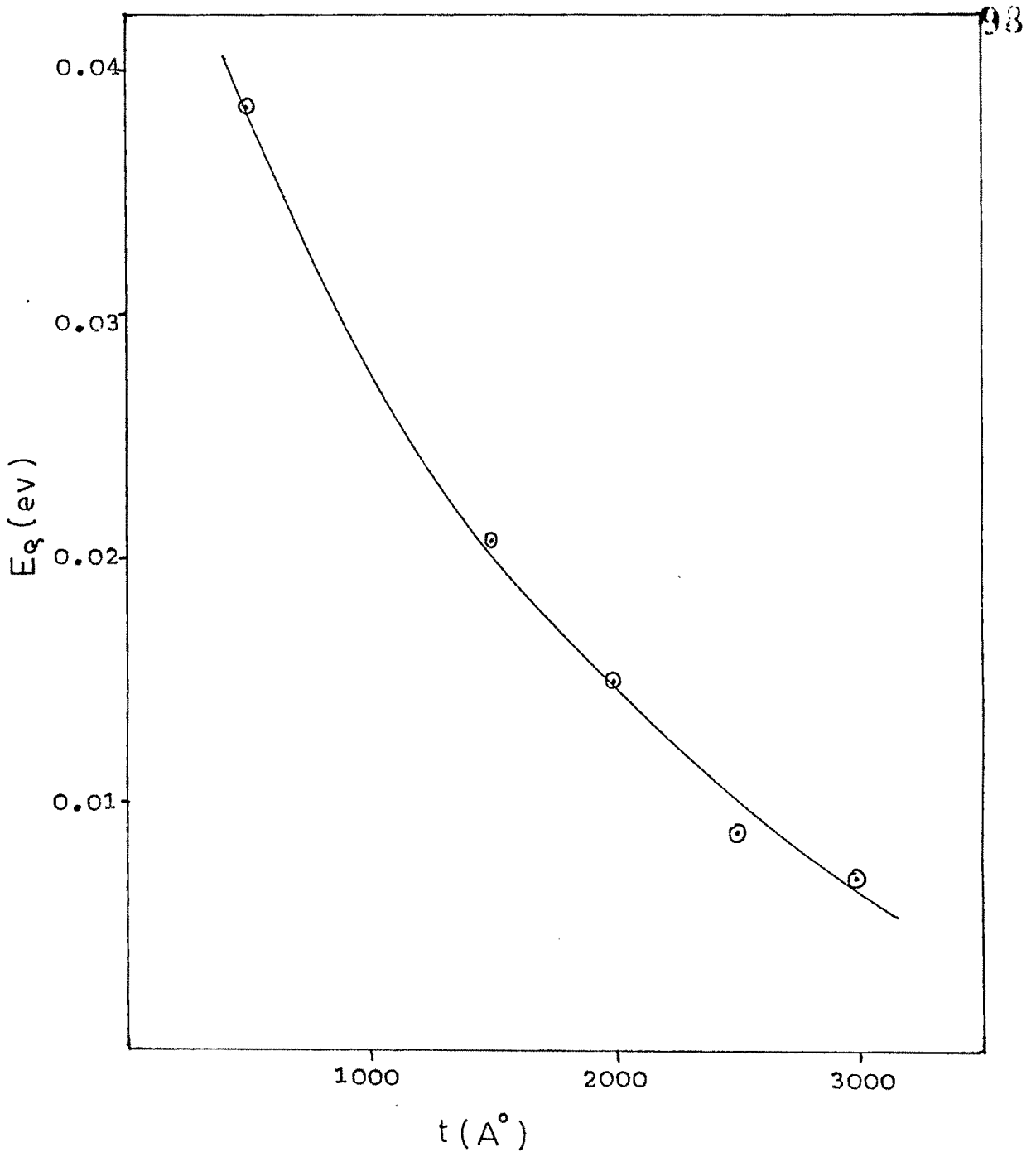


Figure - 12 : Plot of E_g vs t ; SnSe_2 films.
 (substrate temperature 200°C)

Effect of film thickness :

The temperature variation of resistivity of films of different thicknesses (number of layers reacted kept constant) is shown in the plots of $\ln \rho$ vs $1/T$ in Figure - 13. The activation energies obtained from these plots and the room temperature resistivities are shown plotted against the film thickness in Figure - 14 and 15, respectively. It is seen that with the increase in the film thickness, the resistivity and activation energy of the films decrease approaching the bulk values. It is worth while to note here that the resistivity of the compound-evaporated films (thickness 2000 Å, for example) is 13.46 ohm-cm (Figure - 6) while that of solid state reacted films of the same thickness is 0.57 ohm-cm (Figure - 13). For the films of smaller thickness, the resistivity is too high. This may be due to voids and imperfections in the films rendered effective by thickness becoming comparable to or less than the mfp of carriers. Similar situation holds for films where contamination continues as the deposition progresses. It is known that the grain size increases with the film thickness and the smaller the size of the grain, the greater is the activation energy⁽¹⁰⁾.

Thermal Cycling :

It is seen from the graph of resistance vs temperature, shown in Figure - 16, that there is no noticeable change in the resistance of the film, probably indicating no effect on

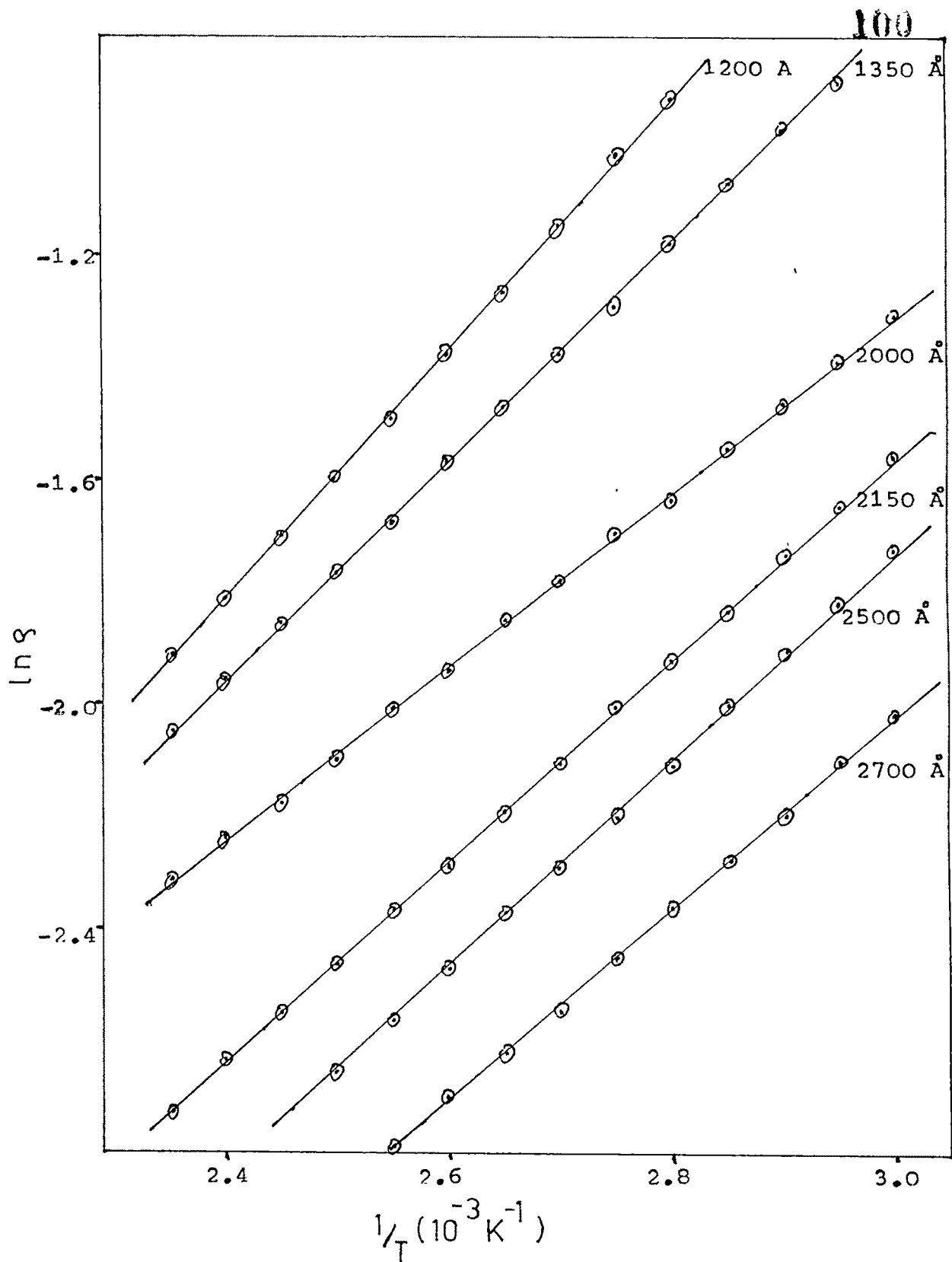


Figure - 13 : Plot of $\ln s$ vs $1/T$; SnSe films (solid state reacted) of indicated thicknesses.

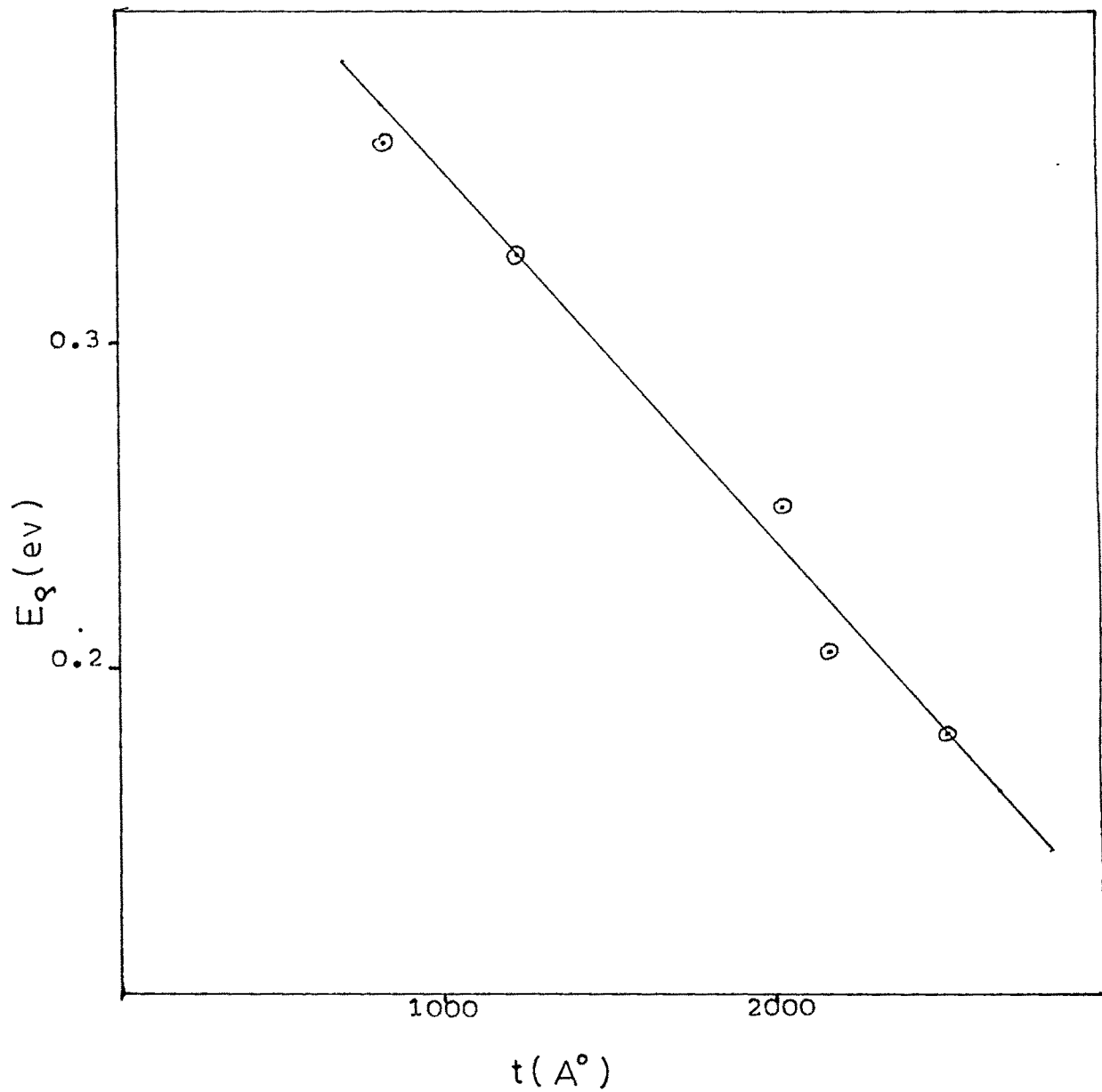


Figure - 14 : Plot of E_g vs t ; SnSe solid state reacted film.

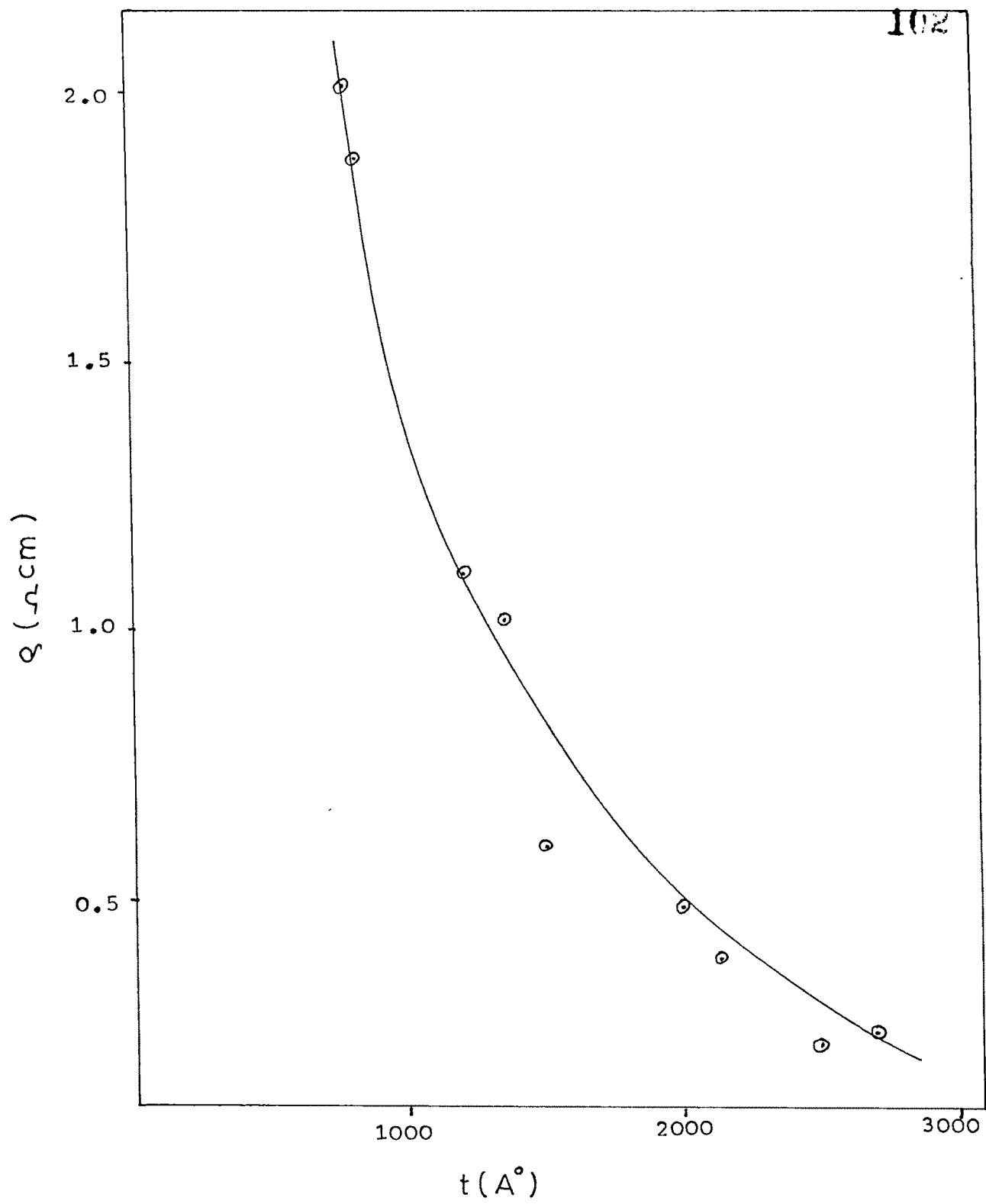


Figure - 15 : Plot of g vs t ; SnSe solid state. reacted film.

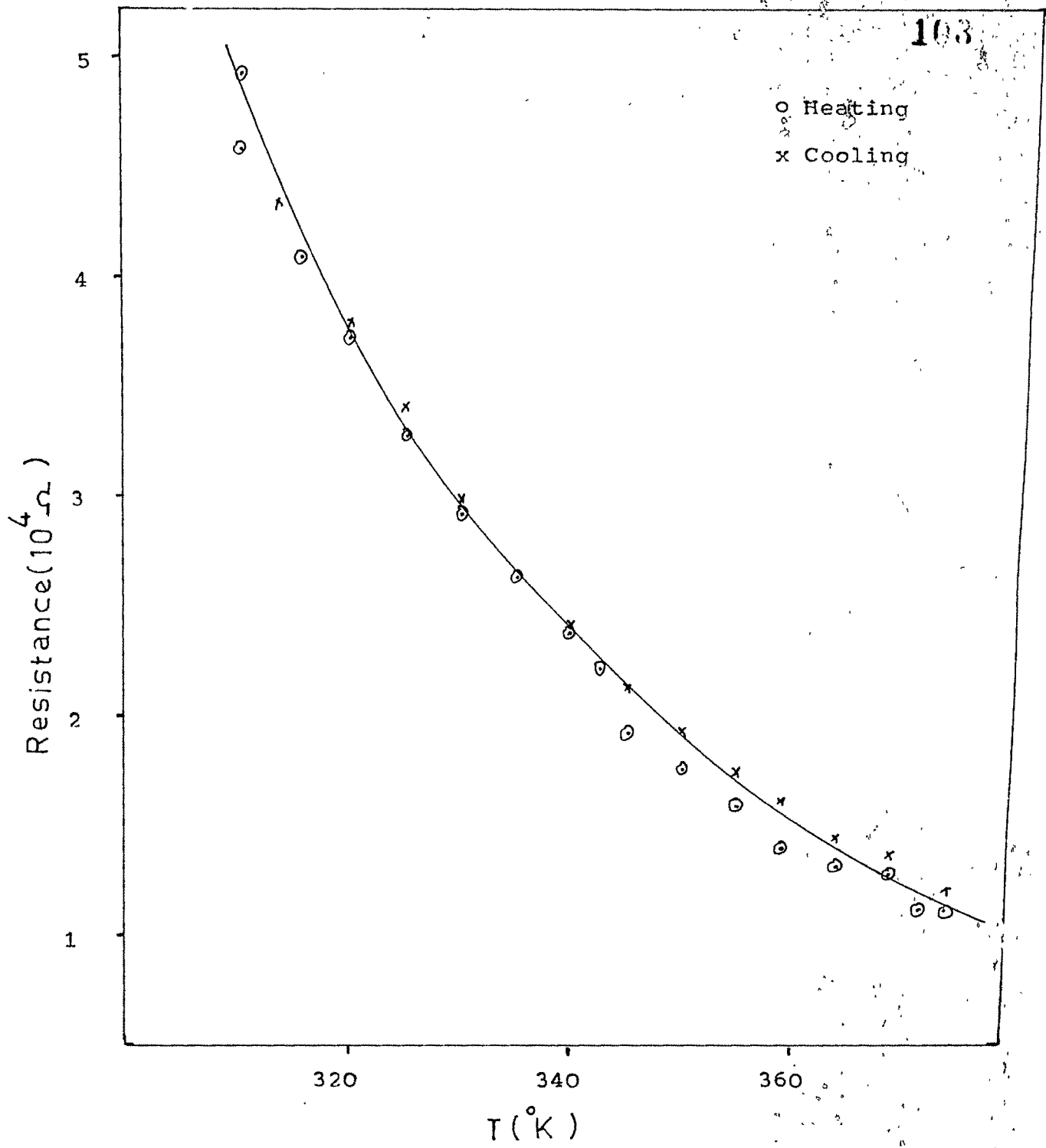


Figure - 16 : Thermal cycling curve ; Resistance vs temperature ; SnSe solid state reacted films (t ~ 2700 Å)

TABLE - 1

Room temperature resistivity and activation energy

Crystal	ρ (ohm-cm)	E_{g_1} (ev)	E_{g_2} (ev)
SnSe	0.21	3.6×10^{-2}	0.11
SnSe ₂	0.41	5.2×10^{-3}	-
SnSe-SnSe ₂ (eutectic)	9.03	7.2×10^{-2}	-

TABLE - 2

Room temperature resistivity and activation energy
of the SnSe solid state reacted films deposited
at various substrate temperatures
($t \sim 1200 \text{ \AA}$)

Sub. temp. (°C)	ρ (ohm-cm)	E_g (ev)
30	1.20	0.16
100	0.40	0.12
150	0.07	0.10

crystallinity of the films by thermal cycling.

Effect of Substrate Temperature :

Films were deposited at various substrate temperatures keeping the thickness and number of layers constant. In Table - 2 are listed the room temperature resistivity and the activation energy of the films. It is seen that the resistivity and activation energy of the films decrease with increasing substrate temperature. The crystallinity of the films is poor at low substrate temperature. The intercrystalline regions in these cases may be wide, offering a high resistance to the motion of carriers. Higher substrate temperatures favour the formation of fewer nucleation centres resulting in larger crystallite size and hence the intercrystalline barriers decrease in size. Thus the behaviour of resistivity at different substrate temperatures is due to essentially uncontrolled nucleation and growth of crystallites which comprise the film. A quantitative explanation has been given on the basis of the Petriz's Barrier Model⁽¹⁹⁾.

The number of layers in the solid state reacted films were varied from 3 to 9, keeping the total film thickness constant, viz. 1200 Å. In Table - 3 are given the room temperature resistivity and activation energy of the films with different number of layers. It is seen that with the increase in the number of layers, the resistivity and activation energy

decrease. It is quite probable that with the increase in number of layers and decrease of individual layer thickness, the reaction occurs more and more uniformly. Hence, the films obtained from a larger number of layers would be more homogeneous and structurally perfect.

3.2.3 Films obtained from SnSe - SnSe₂ eutectic alloys :

EFFECT OF THICKNESS :

Films from 500 Å to 2000 Å thicknesses were subjected to resistivity measurements at different temperatures. The graph of $\ln \rho$ vs $1/T$ for different thicknesses is shown in Figure - 17. It is seen that in this case also, with the increase in the film thickness the resistivity and activation energy both decrease. The resistivity and activation energy for different thicknesses are shown in Figure - 18 and 19, respectively.

Thermal Cycling :

The films were heated to 150°C and cooled to room temperature a number of times, till heating and cooling curves of resistance versus temperature become colinear. A typical curve is shown in Figure - 20. In this case, the rate of heating was about 1 °C/min. The films exhibit fall in resistance by a factor of 100 after 2 cycles. There was no observable effect of further cycling. It should be noted that such pronounced effect of thermal cycling was observed only in

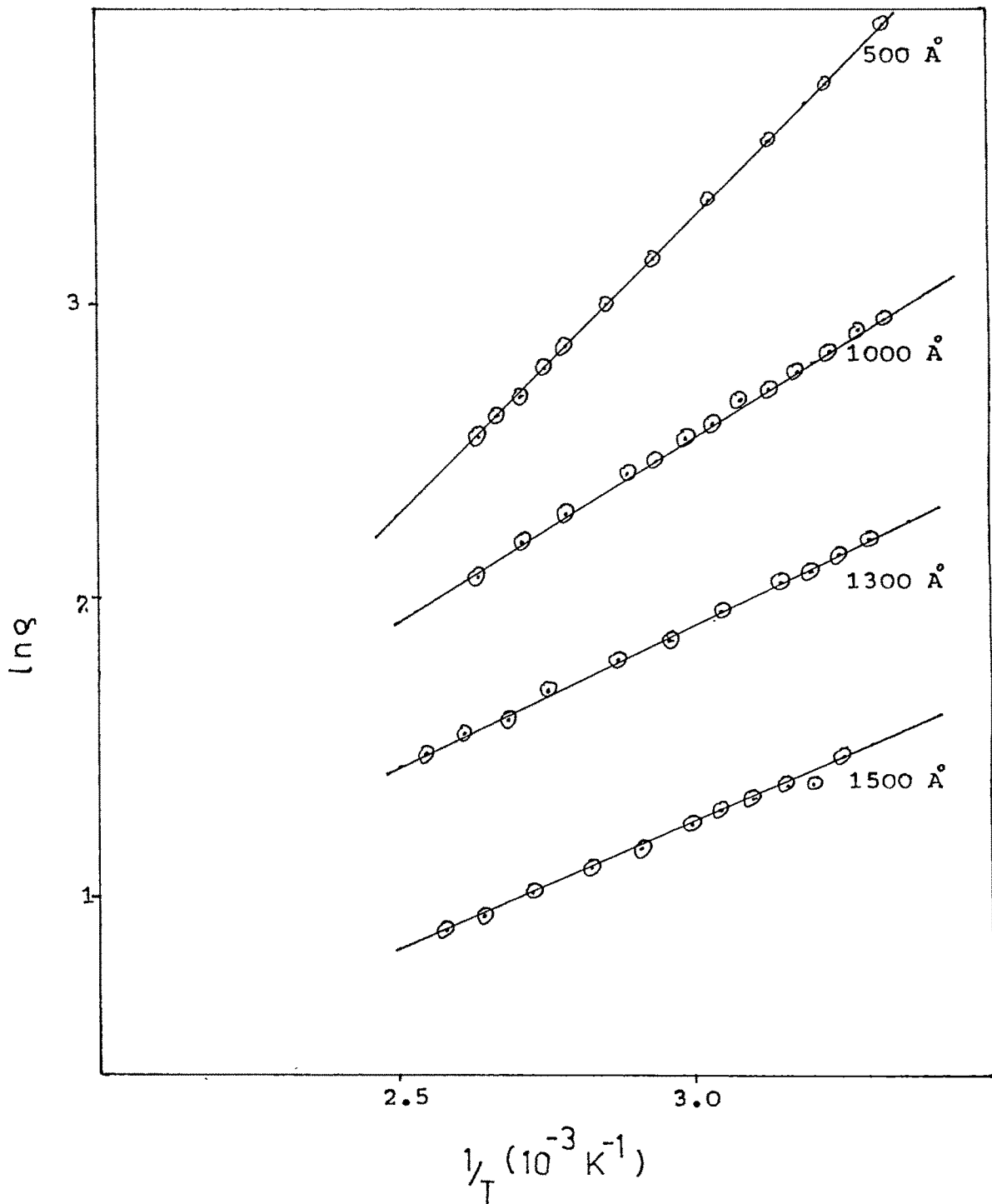


Figure - 17 : Plot of $\ln g$ vs $1/T$; SnSe-SnSe₂ eutectic films.
(room temperature deposition)

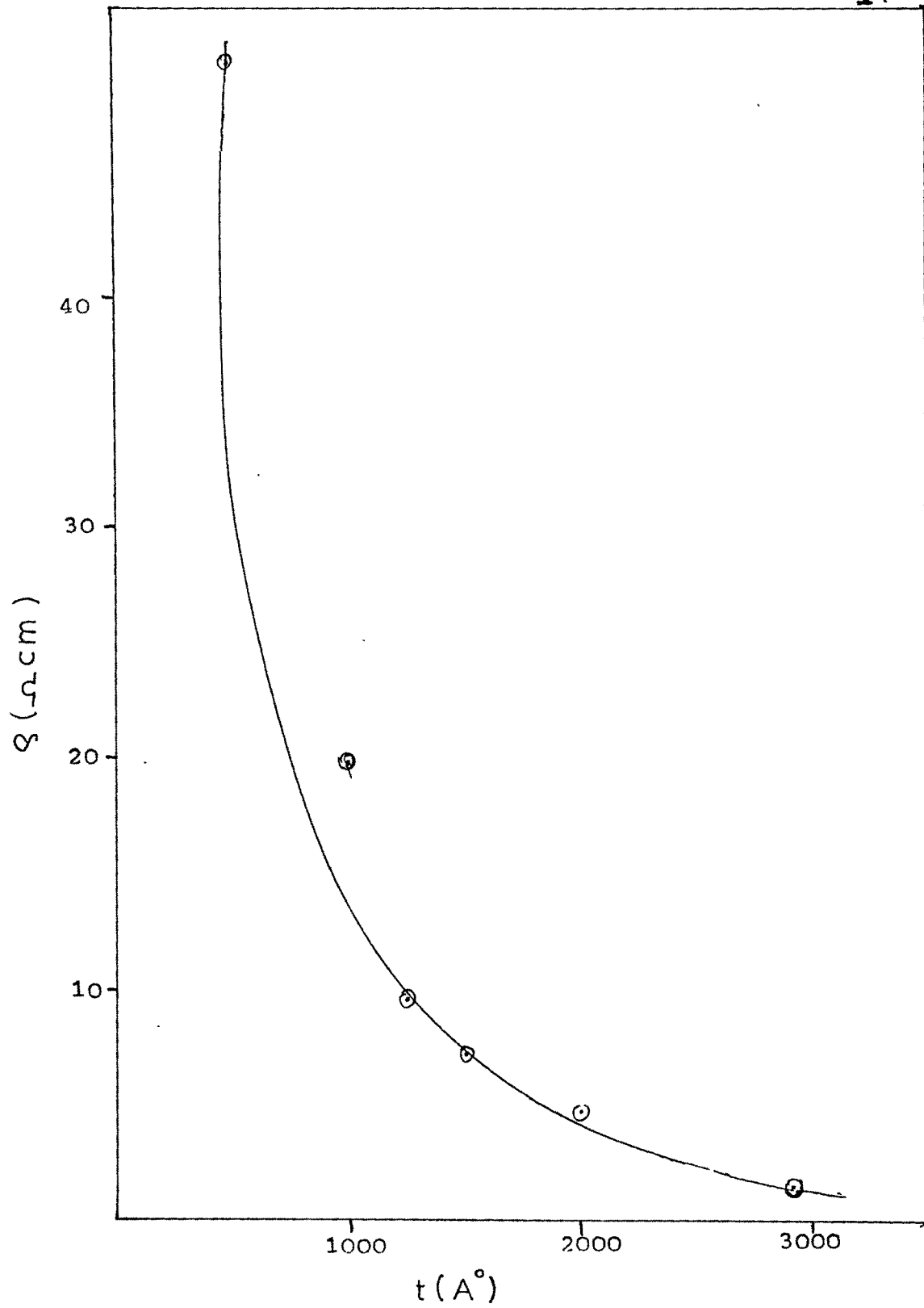


Figure - 18 : Plot of ρ vs t ; SnSe-SnSe₂ eutectic films.
(room temperature deposition)

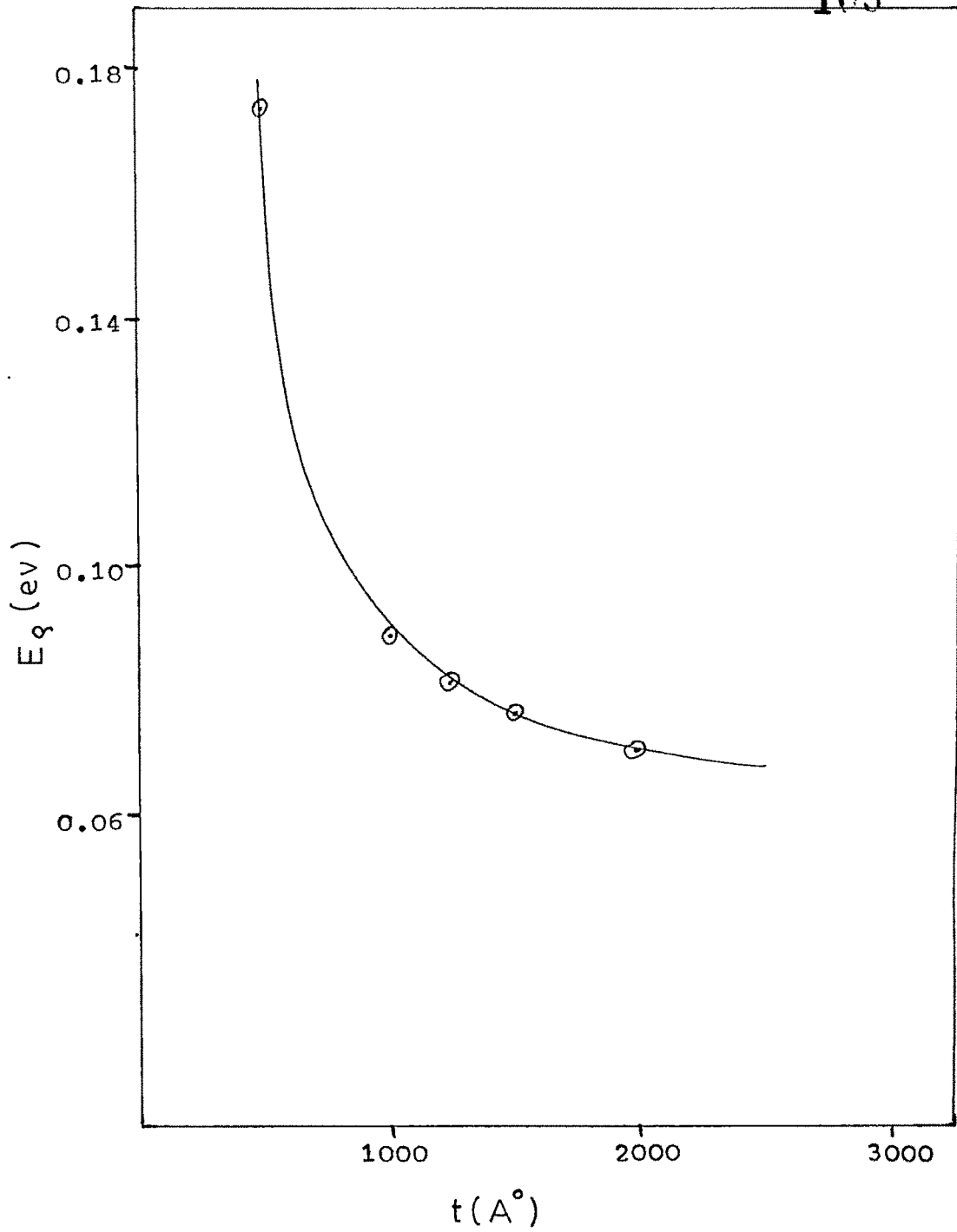


Figure - 19 : Plot of E_g vs t ; SnSe-SnSe₂ eutectic films.
(room temperature deposition)

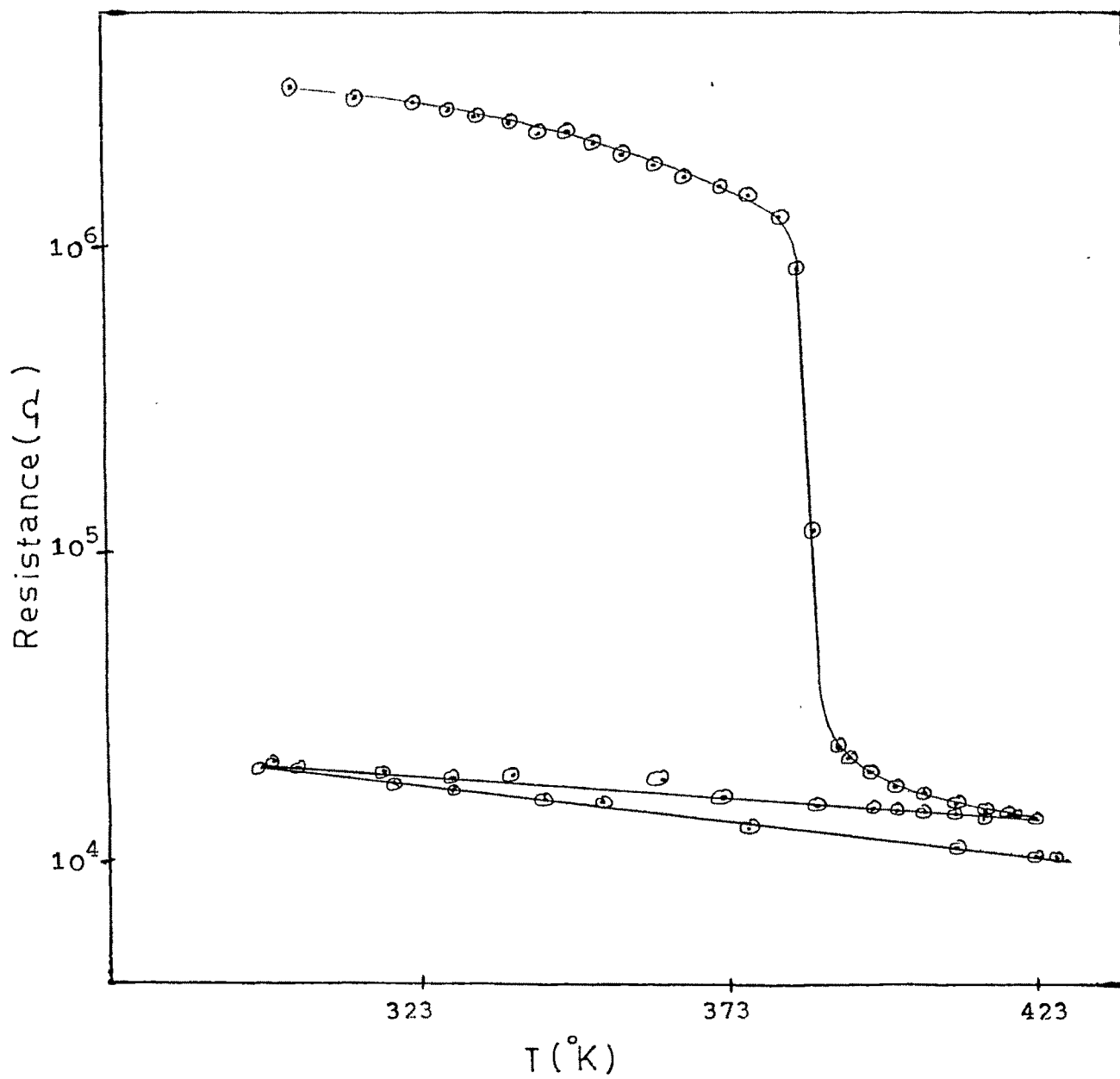


Figure - 20 : Thermal cycling: R vs temperature ; SnSe-SnSe₂ films.

the case of films deposited at room temperature. For films deposited at temperatures higher than 50°C, there was little or no effect of thermal cycling. This may be because of amorphous nature of the films deposited at room temperature. This is indicated by abrupt decrease in resistance, observed in the first heating cycle, which may be associated with the on-set of recrystallization of amorphous films, the onset being at about 100°C in this case. The change in resistance was observed to be highly dependent on the rate of heating. If the heating rate was kept above 1°C/min, it was observed that the resistance decreased in general but the decrease was not systematic.

Effect of Substrate Temperature :

To study the effect of substrate temperature on resistivity, the films (thickness 500 Å) were deposited on glass substrates at various temperatures. The observed resistivity variation with substrate temperature is also indicated in the plots of Figure - 21. The trend is similar to the one observed for the solid state reacted SnSe films. It is seen that with the increase in the substrate temperature the resistivity decreases.

Effect of Annealing :

For studying the annealing effect on resistivity, the films (thickness 500 Å) were deposited on glass substrates and

annealed in vacuum for 3 hrs at different temperatures ranging from 50° to 150°C. The values of resistivity measured at room temperature for films annealed at different temperatures are given in Table - 4. It is seen that the resistivity decreases with increase in anneal temperature. It is known that during the deposition of the film, many structural defects are included in the film. Among such imperfections large contribution to resistivity may arise from vacancies and the vacancy concentration decreases with the annealing temperature. As a result, the resistivity decreases with anneal temperature. Another significant source of electron scattering is the grain boundaries in the film. If the grain size is smaller than the mfp, internal diffuse scattering at surface will increase the resistivity. The transport of electrons across a grain boundary potential may be a thermally activated tunneling process. The annealing process includes changes in the size and the separation of islands in the films and, thereby, rapid changes in the electrical conductivity.

3.3 Hall Measurement :

Hall measurements were tried on SnSe, SnSe₂ and SnSe solid state reacted films. SnSe₂ films and the films deposited from SnSe-SnSe₂ eutectic alloys were of high resistivity and hence it was not possible to measure their Hall coefficient. Goswami's five probe geometry was used for the measurements. Aluminium electrodes were deposited as the probes which are

TABLE - 3

Room temperature resistivity and activation energy of
SnSe solid state reacted films obtained with
different number of layers ($t \sim 1200 \text{ \AA}$)

Layers	ρ (ohm-cm)	E_g (ev)
3	5.5	0.26
5	1.3	0.24
7	1.2	0.16
9	0.3	0.16

TABLE - 4

Room temperature resistivity activation energy of the
SnSe-SnSe₂ eutectic films annealed at
different temperatures ($t \sim 500 \text{ \AA}$)

Anneal. temp. (°C)	ρ (ohm-cm)	E_g (ev)
as grown	51.4	0.18
50	24.5	0.15
100	9.8	0.11
150	6.3	0.10
200	5.2	0.09

ohmic to these films. At the extreme ends, the probes 1 and 2 (as shown in Figure - 22) were connected to a power supply with a digital current meter in series and across the probes 4 and 5, a digital microvoltmeter was connected to measure the voltage. The film was placed between the poles of a strong electromagnet giving a field of about 5 K gauss maximum. The current and voltage were measured with and without the magnetic field. A large number of samples were measured. On average the mobility and carrier concentration of the SnSe solid state reacted films were found to be about $115 \text{ cm}^2/\text{Vs}$ and $2 \times 10^{16} \text{ cm}^{-3}$, respectively. For SnSe films directly evaporated from the compound, they were found to be about $60 \text{ cm}^2/\text{Vs}$ and $4 \times 10^{16} \text{ cm}^{-3}$, respectively.

The Hall mobility and carrier concentrations reported (by Dang Tran Quan) for SnSe film synthesized by solid state reaction, are $59 \text{ cm}^2/\text{Vs}$ and $9.5 \times 10^{16} \text{ cm}^{-3}$, respectively. While for the compound evaporated SnSe films, the mobility and carrier concentration are reported by W. Albers, respectively, to be $100 \text{ cm}^2/\text{Vs}$ and $3 \times 10^{18} \text{ cm}^{-3}$. Thus in this case the mobility of solid state reacted SnSe films is higher than that of directly evaporated films. This together with the decreased carrier concentration implies the method of solid state reaction to be superior to the method of evaporating the compound material.

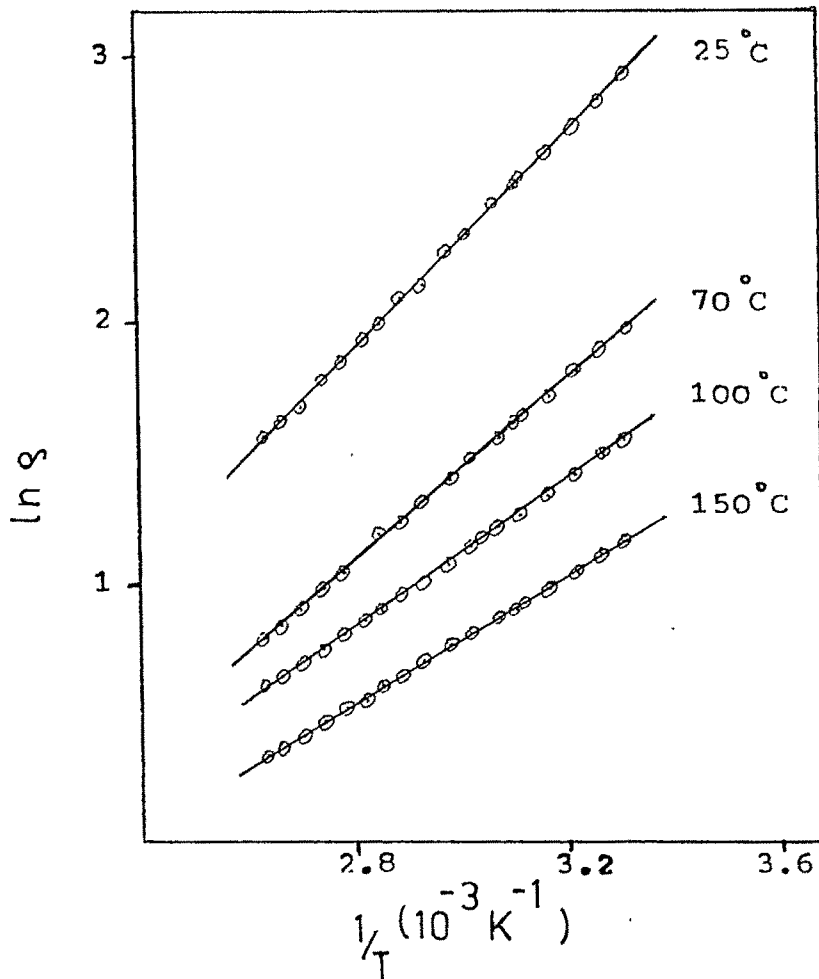


Figure - 21 : Plot of $\ln \rho$ vs $1/T$;
 SnSe-SnSe₂ eutectic
 films deposited at
 various substrate
 temperatures indicated
 ($t \sim 500 \text{ \AA}$)

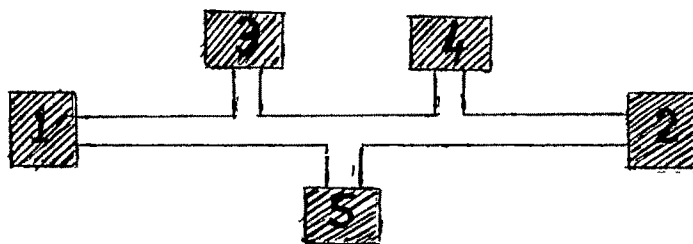


Figure - 22 : Goswami's linear probe
 geometry used for
 Hall measurement.

CONCLUSIONS :

1. The room temperature resistivity of the single crystals of SnSe, SnSe₂ and SnSe-SnSe₂ eutectic are 0.21 ohm-cm, 0.41 ohm-cm and 9.03 ohm-cm, respectively.
2. The resistivities and activation energies of SnSe and SnSe₂ thin films decreased with substrate temperature and film thickness. On an average their resistivity values are of the order of about 15 ohm-cm and 20 ohm-cm.
3. However, among the SnSe₂ films deposited on the three substrates (NaCl, mica and glass), the values obtained for films on NaCl cleavages are the least, viz. about 5 ohm-cm.
4. The resistivity of the SnSe thin films obtained by solid state reaction is quite small, by a factor of about 40 to 50, compared to that of the thin films obtained by evaporation of the compound. Within the range of number of layers reacted, the films with 9 layers have the least resistivity values, of the order of 0.3 ohm-cm.
5. The SnSe solid state reacted films in the present study have a value of resistivity about one-tenth the results

in a previous report.

6. The as-grown films obtained from the SnSe-SnSe₂ eutectic have high resistivity which can be lowered by a factor of about 100 to 200 by thermal cycling upto 150°C.

7. The films obtained from SnSe-SnSe₂ eutectic have resistivity and activation energy decreasing both with the substrate temperature and film thickness. On an average their resistivities are of the order of 30 to 40 ohm-cm.

REFERENCES :

1. L. Valdes : Proc. IRE 42 (1954) 420.
2. A. Goswami and S.M. Ojha : Thin Solid Films 16 (1973) 187.
3. V.P. Bhatt, K. Gireesan and G.R. Pandya : J. of Cryst. growth 96 (1989) 649.
4. Y.G.Yu, A.S. Yue and O.M. Stafsudd Jr.: J. of Cryst. growth 54 (1981) 248.
5. G.Domingo, R.S. Itoga and C.R. Kannerwurf : Phy. Rev. 143 (1966) 143.
6. W. Albers and J. Verberkt : Journal of Mat. Science 5 (1970) 24.
7. Dang Tran Quan : Phys. Stat Sol. (a) 86 (1984) 421.
8. Dan Tran Quan : Thin Solid Films 149 (1987) 197.
9. A.H.Wilson : Theory of metals, Cambridge University Press, New York, (1958).
10. K.L. Chopra : Thin film phenomena, McGraw Hill book Company, New York (1969).

11. L.J. Van der Pauw : Philips Res. Repts. 13 (1958) 1.
12. D.M. Chizhikov and V.P. Shchastlivyi : Selenium and Selenides, Collet's Publisher Ltd. London 1968 301.
13. C.Dunlop Jr. : An introduction to semiconductor : John Wiley and Sons, Inc. New York (1957).
14. R.H. Bube : Electrons in Solids Academic Press, Inc. New York, 1988.
15. V.P. Bhatt, K.Gireesan and C.F. Desai : Cryst. Res. Technol 24 (1989) 187.
16. A.K. Garg, A.K. Jain and O.P. Agnihotri : Ind. Journal of pure and Appl Phy. 21 (1983) 276.
17. V.P. Bhatt, K.Gireesan : J. of Mat. Sci letters 9 (1990) 362.
18. A.M. Elkovashy : J of Phy. Chem. Sol. 47 (1986) 497.
19. Petritzs : Phys. Rev. 104 (1956) 1508.